Supporting Information

Perylene Diimide Isomers Containing Simple sp^3-Core for Non-Fullerene-based Polymer Solar Cells

Gi Eun Park,[a] Suna Choi,[a] Dae Hee Lee,[a] Mallesham Godumala,[a] Mohammad Afsar Uddin,[b] Han Young Woo,[a] Min Ju Cho*[a] and Dong Hoon Choi*[a]

[a] Dept. of Chemistry, Research Institute for Natural Sciences, Korea University, 5 Anam-dong, Sungbuk-gu, Seoul 136-701, Korea

[b] Dept. of Nanofusion Engineering, Dept. of Cogno-Mechatronics Engineering, Pusan National University, Miryang 627-706, Korea

Measurement: An elemental analyzer (Thermo Scientific Flash 2000 (Thermo Fisher Scientific)) was used for determination of the elemental composition (C, H, N, and S) of the final compounds (*t*-OCP, *t*-OCP-m, *t*-MCP, *c,t*-MCP-m, and *t*-PCP). ^{1}H NMR spectroscopy (Bruker 500 MHz) was used to determine the chemical structures of the synthesized compounds. The masses of the synthesized compounds were determined by matrix-assisted laser desorption ionization time of flight (MALDI-TOF) mass spectrometry (LRF20, Bruker Daltonics).

The optical properties of the isomers in the solution and film states (λ = 190−1100 nm) were characterized by using a UV-vis absorption spectrophotometer (HP 8453 photodiode array). The samples in the film state were prepared by the spin-coating method using a 0.7 wt% chloroform solution of the respective small molecules on washed glass substrates.

Cyclic voltammetry (CV, eDAQ EA161) was used to examine the electrochemical properties of the small molecules. The desired thin film on a Pt plate was prepared by drop-casting from a chloroform solution, while the 0.10 M electrolyte solution was prepared by dissolving tetrabutylammonium hexafluorophosphate (Bu_4NPF_6) in acetonitrile with a Pt wire and Ag/AgCl as the counter and reference electrodes, respectively.

Two-dimensional GI-XRD measurements (9A (U-SAXS) were performed at the 9A beamline in the Pohang Accelerator Laboratory (PAL)); the energy, pixel size, wavelength, and scanning interval at the 9A beamline were 11.075 keV, 79.59 μm, 1.11946 Å, and 2θ = 0°–20°, respectively. The scattering vectors, q_{xy} and q_z were respectively parallel and perpendicular to the substrate. The film samples for the GI-XRD analysis were fabricated by spin coating the small molecule solution and blending the solution of small molecules and PPDT2FBT on a UVO-ozone pretreated wafer.

Atomic force microscopy (AFM, XE-100 Advanced Scanning Prove Microscope, PSIA) was used to examine the surface morphologies of the films; the microscope was equipped with a silicon cantilever that was used in tapping mode. The samples for the AFM measurements were fabricated in the same manner as used for the photovoltaic devices. Transmission electron microscopy (TEM, Tecnai G2F30 TEM (FEI Inc.) at an accelerating voltage of 300 kV) was used to observe the internal morphology of the blend films, and the samples were fabricated on a carbon-coated copper grid.

Space-charge-limited current (SCLC) method for measuring charge carrier mobility: The modified Mott-Gurney equation was used to determine the hole and electron carrier mobilities by fitting the *J-V* curves to the near quadratic region.

The respective structures of the hole only devices (HODs) and electron only devices (EODs) were ITO/PEDOT:PSS/active layer/Au and ITO/ZnO/active layer/LiF/Al. Each active layer was fabricated from the PPDT2FBT:n-type small molecule blend solution (1.5 $mg \cdot mL^{-1}$) in chlorobenzene with 6 vol% DPE as an additive. The thickness of all the active layers was 110 ± 5 nm. After spin-coating the solution, Au or LiF/Al was deposited on the top of the blend film under vacuum.

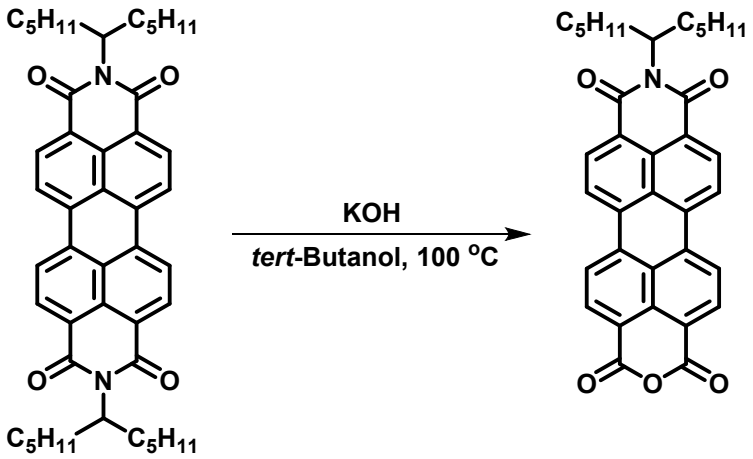

PDI5 **M1**

Scheme S1. Synthesis of perylene monoimido anhydride (M1).

Synthesis of M1

PDI5 (2 g, 2.86 mmol) and KOH (6 g, 0.11 mol) were dissolved in 150 mL of degassed *tert*-butanol in a 250 mL two-neck round bottom flask. The flask was stirred under a nitrogen atmosphere at 100 °C for 10 min. The resultant mixture was poured into a solution of CH_3COOH (100 mL) and HCl (conc.) (50 mL) at 0 °C and stirred for 10 min. The precipitates

were filtered and washed with MeOH several times. The residue was purified by column chromatography (eluent: MC and MC with EA) to obtain the product in 87% yield (1.36 g).

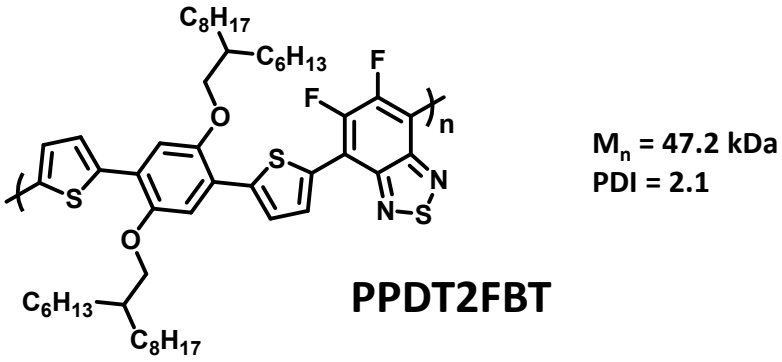

Scheme S3. The structure of donor polymer, PPDT2FBT.

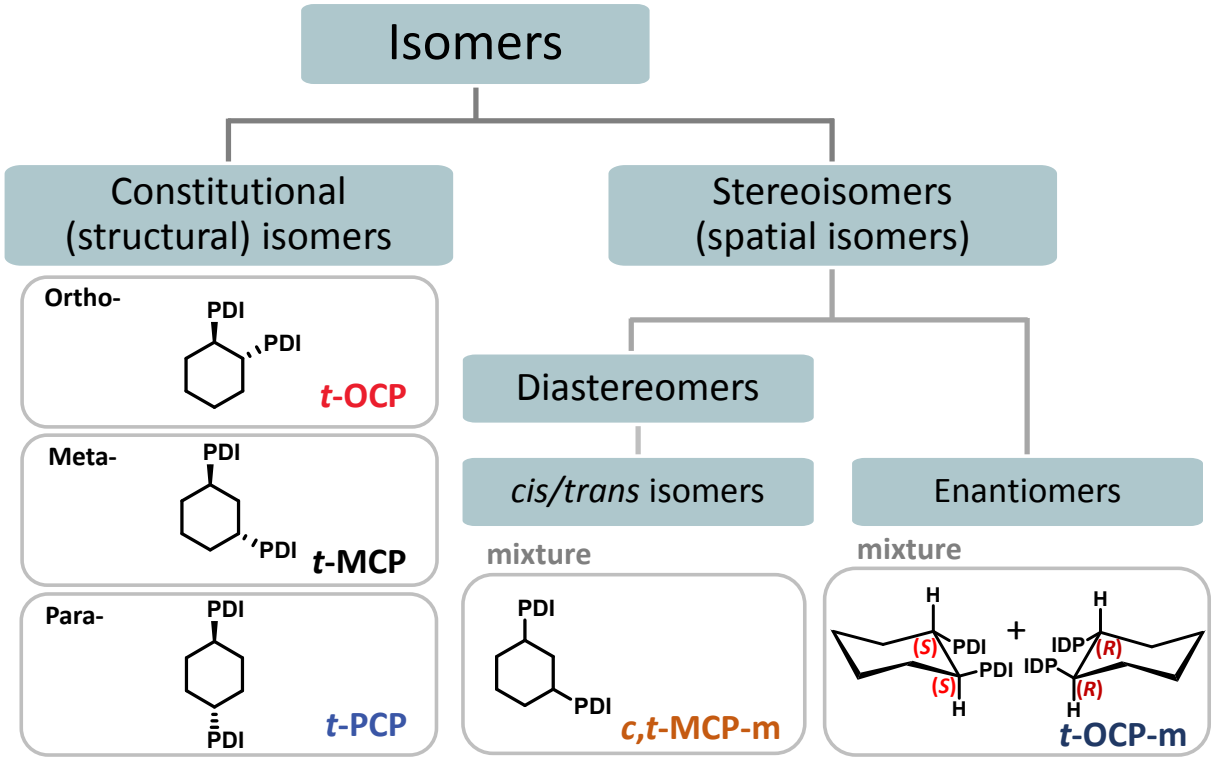

Fig. S1 Classification of PDI-containing isomers.

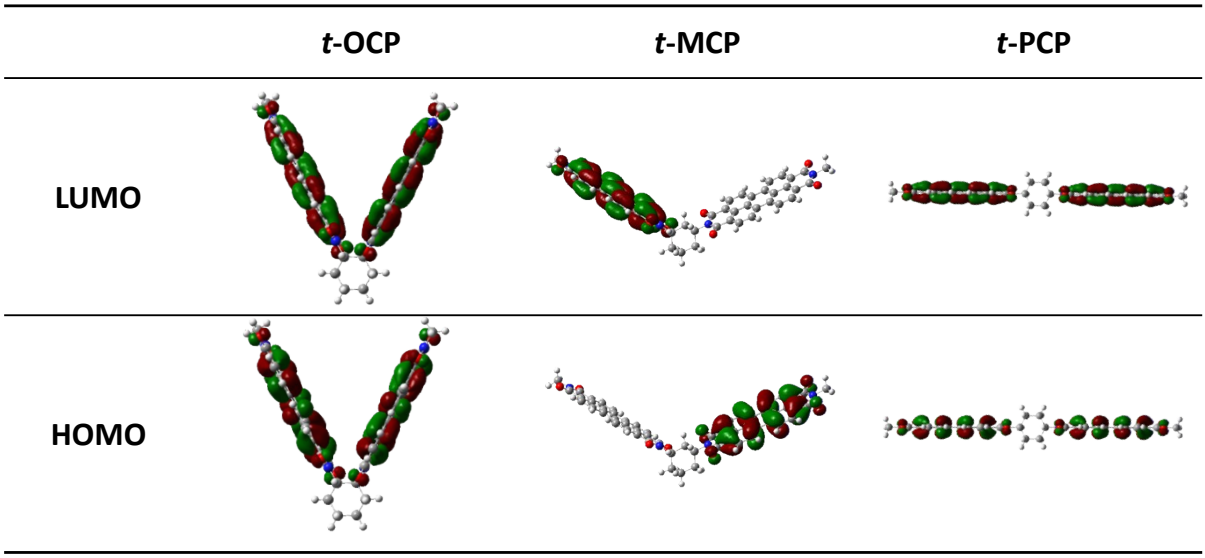

Fig. S2. Molecular structures and DFT calculations of *t*-OCP, *t*-MCP, and *t*-PCP energy levels using B3LYP/6-31G(d).

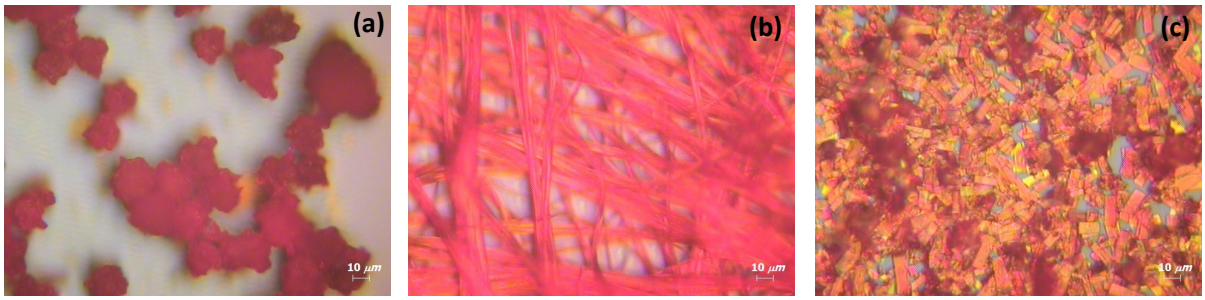

Fig. S3 Images of crystallites of (a) *t*-OCP, (b) *t*-MCP, and (c) *t*-PCP.

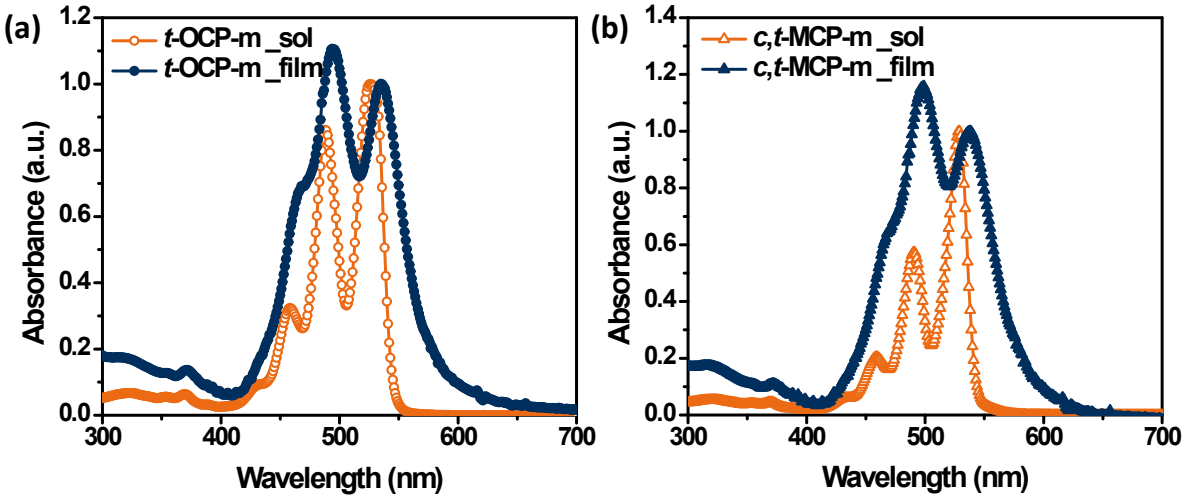

Fig. S4 UV-vis absorption spectra of (a) *t*-OCP-m and (b) *c*,*t*-MCP-m: solution and film.

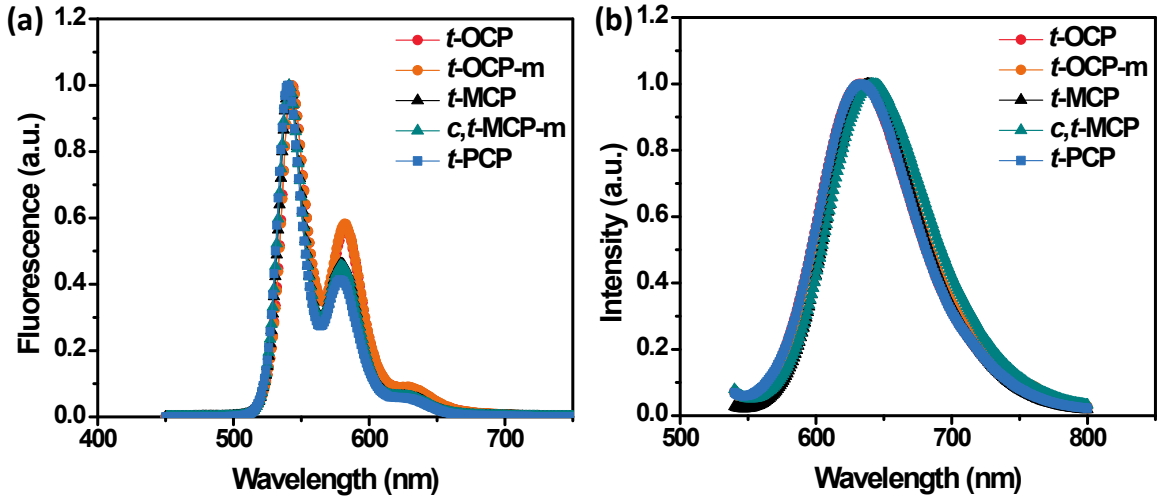

Fig. S5 PL spectra of five isomers. (a) Chloroform solutions and (b) film states.

Table S1. Optical properties of *t*-OCP, *t*-OCP-m, *t*-MCP, *c*,*t*-MCP-m, and *t*-PCP

Acceptor	Absorption		Emission	
	λ_{peak}[a] [nm]	λ_{peak}[b] [nm]	λ_{em}[a] [nm]	λ_{em}[b] [nm]
***t*-OCP**	526	535	543	633
***t*-OCP-m**	526	535	543	636
***t*-MCP**	529	536	541	639
***c*,*t*-mCP-m**	529	536	541	642
***t*-PCP**	526	536	540	633

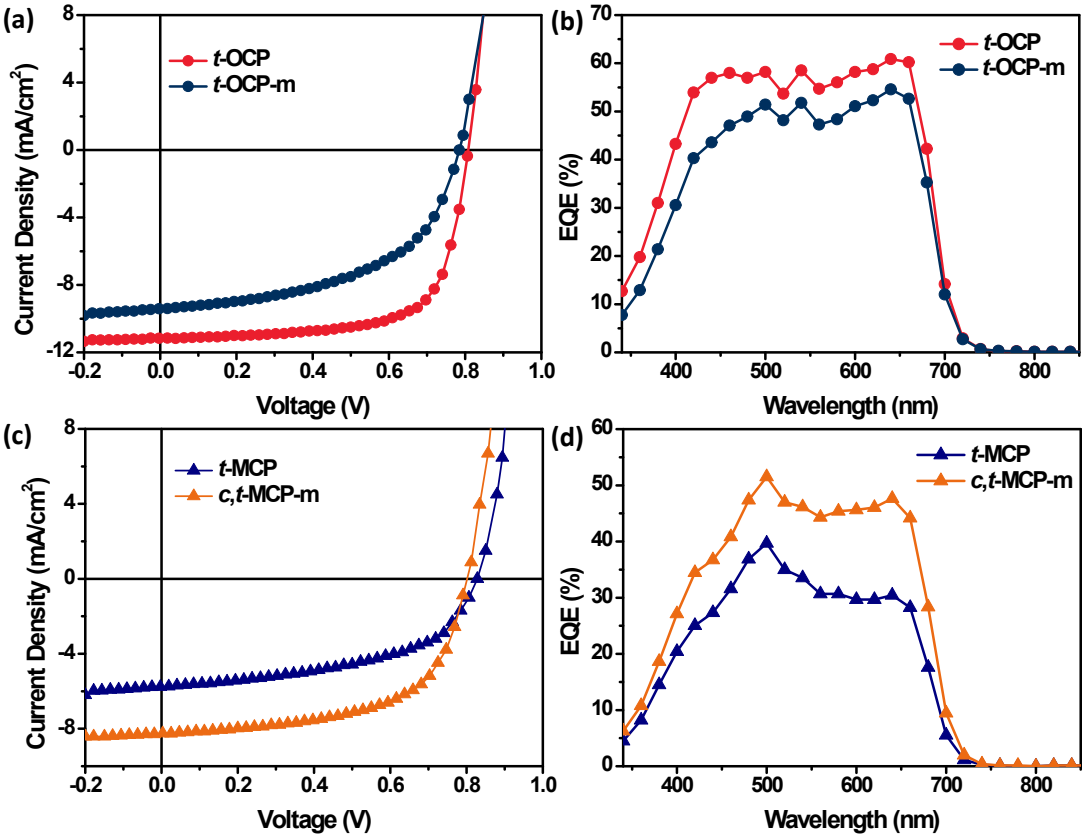

Fig. S6 Current density–voltage (*J*–*V*) characteristics and external quantum efficiency (EQE) spectra of PSCs based on (a) *t*-OCP and *t*-OCP-m and (b) *t*-MCP and *c,t*-MCP-m. Inverted solar cell: ITO/ZnO/active layer/MoO_3/Ag.

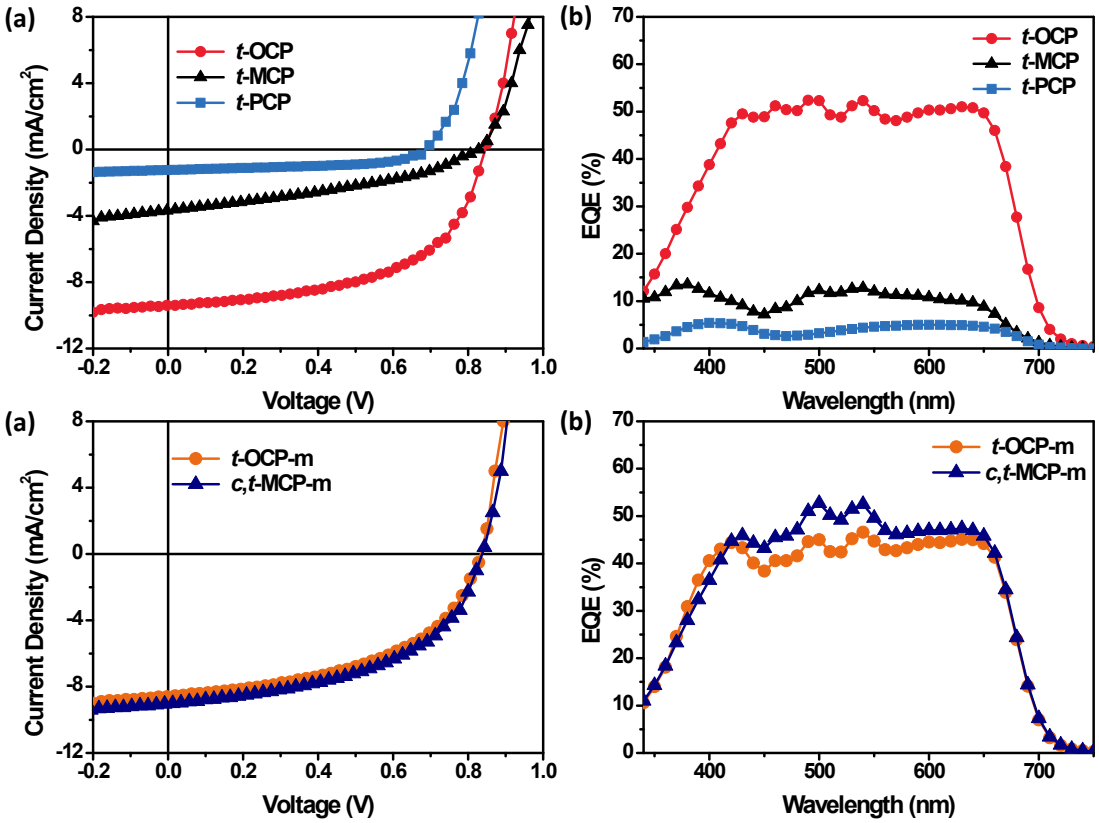

Fig. S7 (a) Current density–voltage (*J*–*V*) characteristics and (b) external quantum efficiency (EQE) spectra of PSCs without solvent additive. Inverted solar cell: ITO/ZnO/active layer/MoO_3/Ag.

Table S2. Performance of PSC devices fabricated with *t*-OCP, *t*-OCP-m, *t*-MCP, *c*,*t*-MCP-m, and *t*-PCP (chlorobenzene without additive)

Acceptor	V_{oc} [V]	J_{sc} [mA·cm^{-2}]	FF	PCE (%)
t-OCP	0.86	9.40	53.84	4.37
t-OCP-m	0.83	8.58	50.12	3.58
t-MCP	0.84	3.67	35.71	1.10
c,t-mCP-m	0.84	9.11	50.70	3.88
t-PCP	0.69	1.24	54.12	0.46

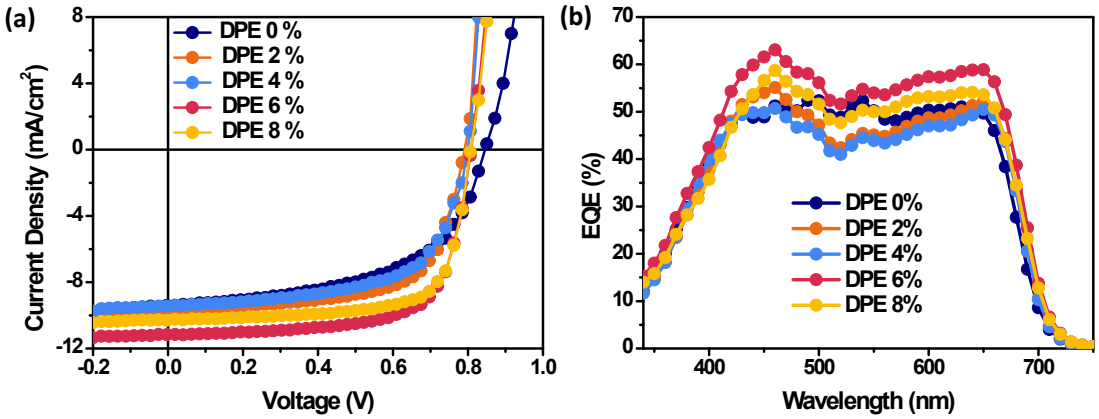

Fig. S8 (a) Current density–voltage (*J*–*V*) characteristics and (b) external quantum efficiency (EQE) spectra of device using *t*-OCP:PPDT2FBT blends as active layer depending on the amount of DPE.

Table S3. Performance of the PSC devices fabricated with *t*-OCP:PPDT2FBT depending on the amount of the additive

Additive	V_{oc} [V]	J_{sc} [mA·cm^{-2}]	FF	PCE (%)
DPE 0%	0.86	9.40	53.84	4.37
DPE 2%	0.80	9.65	65.59	5.03
DPE 4%	0.81	9.43	61.02	4.69
DPE 6%	0.81	11.17	68.86	6.23
DPE 8%	0.81	10.27	70.12	5.83

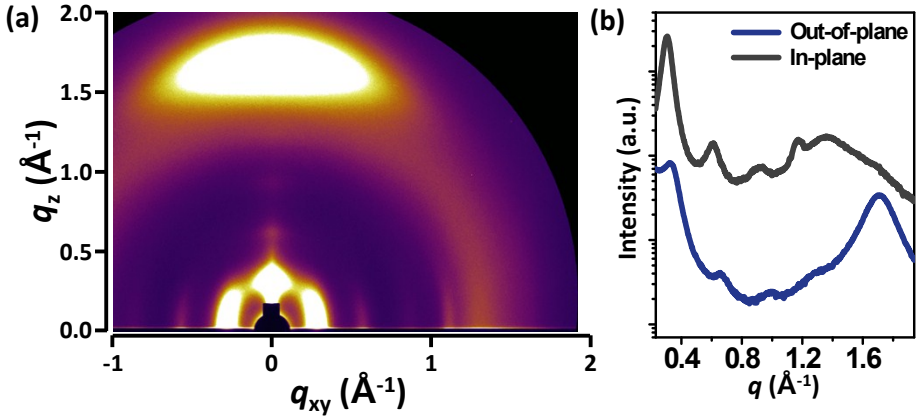

Fig. S9 (a) 2D GI-XRD patterns of PPDT2FBT and (b) 1D out-of-plane (dark blue) and in-plane (gray) profiles extracted from GI-XRD.

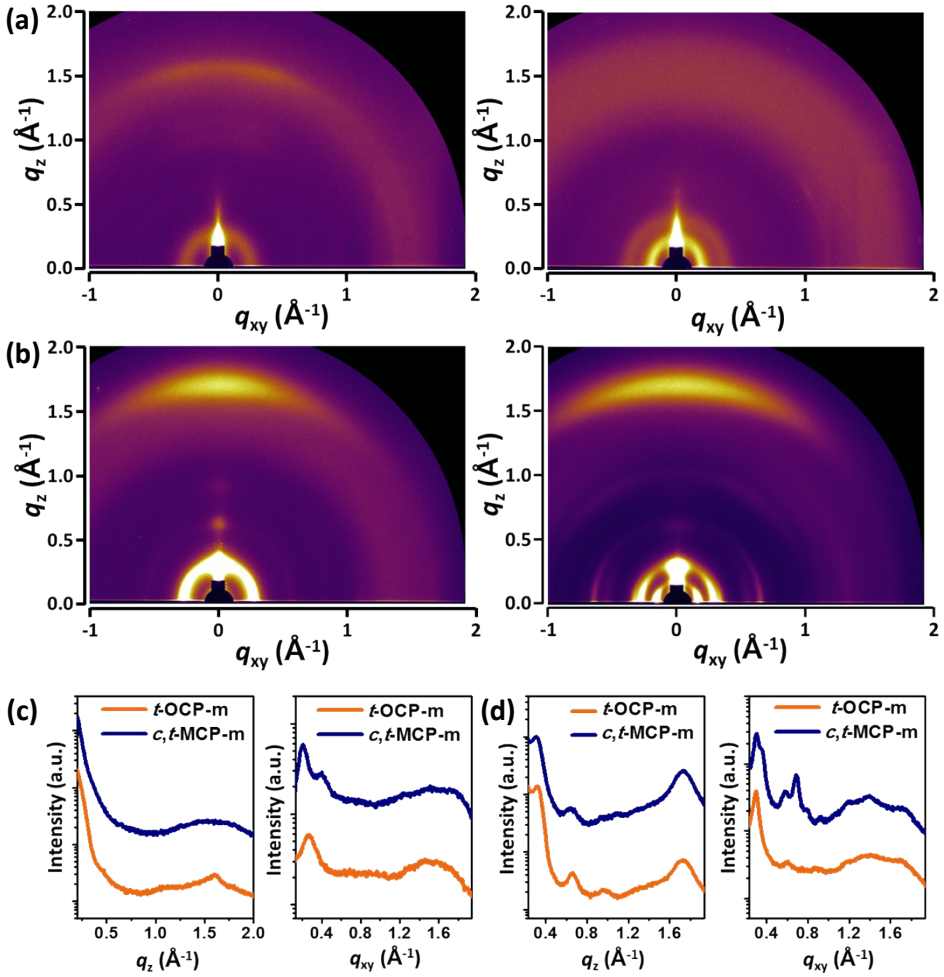

Fig. S10 2D GI-XRD patterns of (a) thin film of *t*-OCP-m and *c*,*t*-MCP-m and (b) blend film of PPDT2FBT:*t*-OCP-m and PPDT2FBT:*c*,*t*-MCP-m. (c) Out-of-plane and in-plane XRD patterns of *t*-OCP-m (green) and *c*,*t*-MCP (blue) thin films. (d) Out-of-plane and in-plane XRD patterns of *t*-OCP-m (green) and *c*,*t*-MCP (blue) blend films with PPDT2FBT.

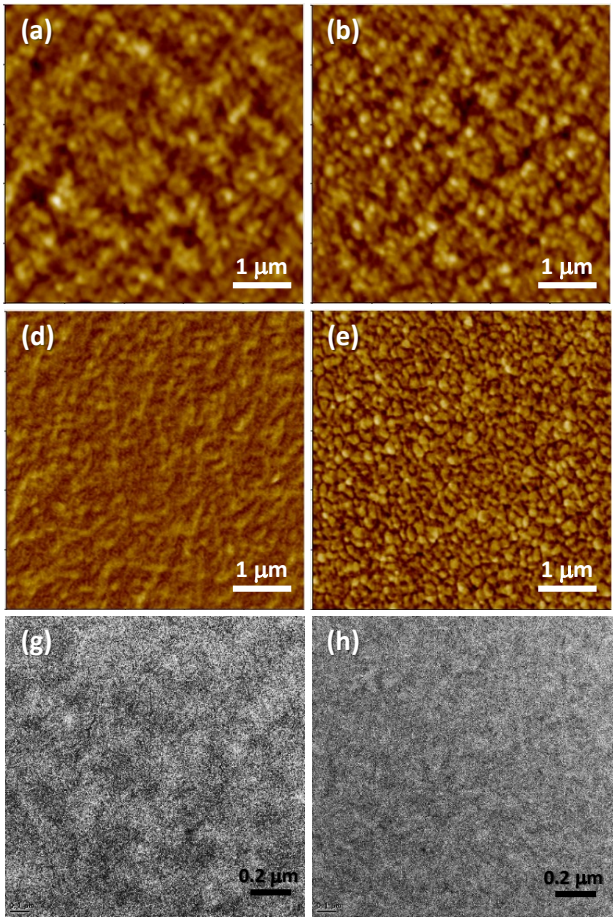

Fig. S11 AFM height images (5 µm × 5 µm) of the blend films: topographical images of (a) t-OPCP-m and (b) *c*,*t*-MCP-m blend films with PPDT2FBT; phase images of (c) *t*-OCP-m and (d) *c*,*t*-MCP-m blend films with PPDT2FBT. TEM images of the blend films of (e) *t*-OCP-m and (f) *c*,*t*-MCP-m with PPDT2FBT.

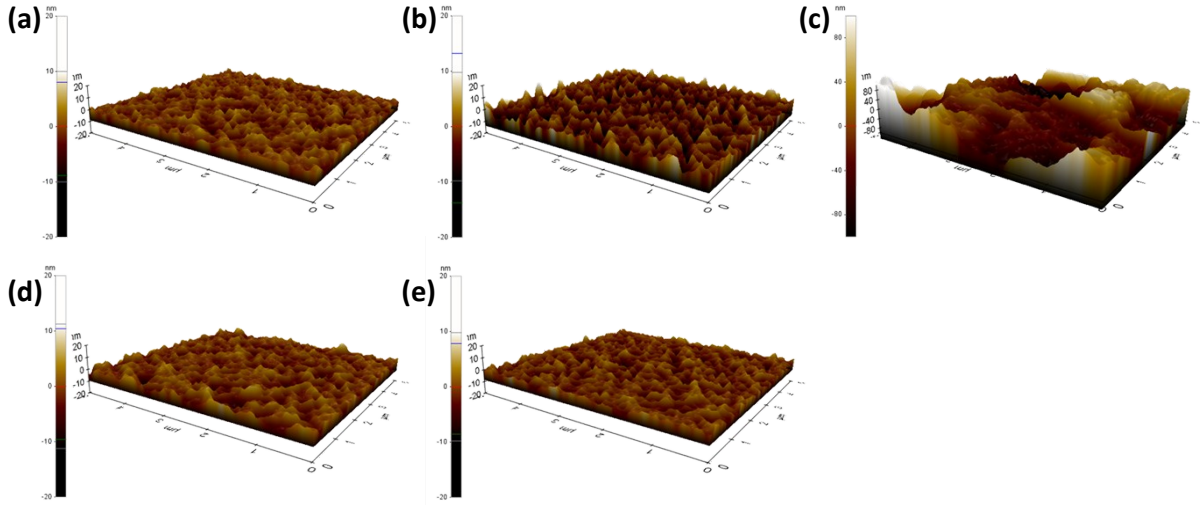

Fig. S12 AFM height 3D-images (5 µm × 5 µm) of blend films: (a) PPDT2FBT:*t*-OCP, (b) PPDT2FBT:*t*-OCP-m, (c) PPDT2FBT:*t*-MCP, (d) PPDT2FBT:*c*,*t*-MCP-m, and (e) PPDT2FBT:*t*-PCP.

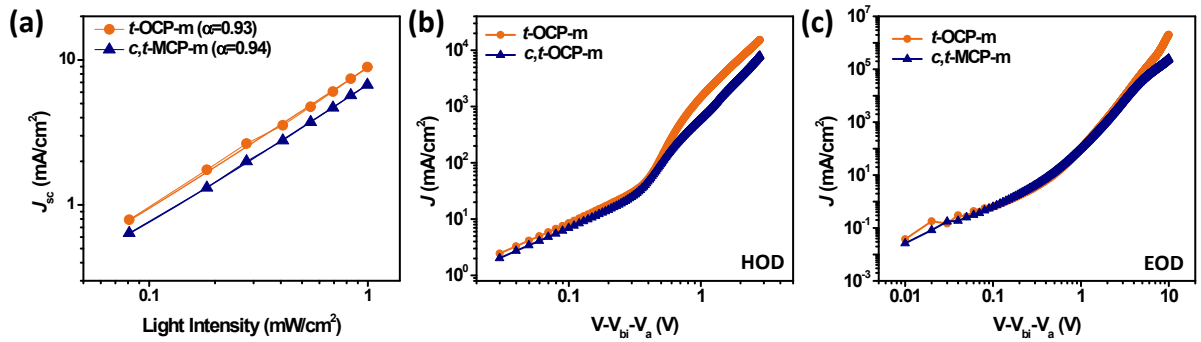

Fig. S13 (a) Photocurrent density (J_{sc}) versus light intensity of optimized devices. Space-charge-limited *J*-*V* characteristics of all blend films under dark conditions for (b) hole-only and (c) electron-only devices of *t*-OCP-m and *c*,*t*-MCP-m.

Table S4. Measured electron and hole mobility of SCLC devices bearing five isomer blends with PPDT2FBT

	μ_h [cm^2/V s]	μ_e [cm^2/V s]	μ_h/μ_e
***t*-OCP**	6.16 x 10^{-5}	5.23 x 10^{-5}	1.18
***t*-OCP-m**	1.21 x 10^{-4}	1.55 x 10^{-5}	7.81
***t*-MCP**	4.35 x 10^{-5}	4.37 x 10^{-6}	9.95
***c*,*t*-MCP-m**	5.60 x 10^{-5}	1.86 x 10^{-5}	3.01
***t*-PCP**	2.21 x 10^{-4}	3.08 x 10^{-5}	7.18